

Helquat Dyes: Helicene-like Push–Pull Systems with Large Second-Order Nonlinear Optical Responses

Benjamin J. Coe,^{*,†} Daniela Rusanova,[†] Vishwas D. Joshi,[‡] Sergio Sánchez,[†] Jan Vávra,[‡] Dushant Khobragade,[‡] Lukáš Severa,[‡] Ivana Císařová,[§] David Šaman,[‡] Radek Pohl,[‡] Koen Clays,^{||} Griet Depotter,^{||} Bruce S. Brunschwig,[⊥] and Filip Teplý^{*,‡}

[†]School of Chemistry, University of Manchester, Oxford Road, Manchester M13 9PL, United Kingdom

[‡]Institute of Organic Chemistry and Biochemistry, Academy of Sciences of the Czech Republic, v.v.i., Flemingovo n. 2, 166 10 Prague 6, Czech Republic

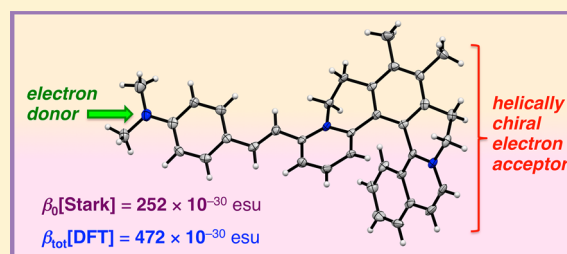
[§]Department of Inorganic Chemistry, Charles University, Hlavova 2030/8, 128 43 Prague 2, Czech Republic

^{||}Department of Chemistry, University of Leuven, Celestijnenlaan 200 D, Leuven B-3001, Belgium

[⊥]Molecular Materials Research Center, Beckman Institute, MC 139-74, California Institute of Technology, 1200 East California Boulevard, Pasadena, California 91125, United States

Supporting Information

ABSTRACT: Helquat dyes combine a cationic hemicyanine with a helicene-like motif to form a new blueprint for chiral systems with large and tunable nonlinear optical (NLO) properties. We report a series of such species with characterization, including determination of static first hyperpolarizabilities β_0 via hyper-Rayleigh scattering and Stark spectroscopy. The measured β_0 values are similar to or substantially larger than that of the commercial chromophore *E*-4'-(dimethylamino)-*N*-methyl-4-stilbazolium. Density functional theory (DFT) and time-dependent DFT calculations on two of the new cations are used to probe their molecular electronic structures and optical properties. Related molecules are expected to show bulk second-order NLO effects in even nonpolar media, overcoming a key challenge in developing useful materials.



INTRODUCTION

Manipulating light via molecular nonlinear optical (NLO) effects¹ is useful in areas like THz wave generation for bioanalysis, security scanning, and space communication.² Pyridinium salts like *E*-4'-(dimethylamino)-*N*-methyl-4-stilbazolium tosylate (DAST, Scheme 1a)^{3,4} are among the best organic NLO materials. Normally, a polar bulk structure is required if the molecular first hyperpolarizability β is to lead to a nonzero value of the second-order NLO susceptibility $\chi^{(2)}$. Second harmonic generation (SHG) is the most immediately useful and widely studied second-order NLO effect.

Recently, new diquat chromophores were introduced (Scheme 1b)⁵ with nonresonant β responses (β_0) larger than that of the DAS⁺ cation. Furthermore, a [6]helicene bisquinone derivative shows very large SHG in Langmuir–Blodgett films.⁶ However, the structural motifs of cationic styryl dyes and helicenes have never been combined for NLO purposes. Indeed, azahelicene dyes⁷ are largely overlooked except in reports from the groups of Lacour⁸ and Arai.⁹ Their NLO properties have not been reported. Importantly, a helical-conjugated molecule has a high nondipolar β tensor component β_{xyz} ; this can give a large $\chi^{(2)}$ in even a nonpolar material, circumventing a key challenge in creating useful substances. Recently, we introduced helquats,¹⁰ and reported the prominent chiroptical

properties of helquat dyes.^{10a} Here, we describe new chromophores of this type (Scheme 1c) and use hyper-Rayleigh scattering (HRS), Stark spectroscopy, and density functional theory (DFT) to assess their second-order NLO responses.

RESULTS AND DISCUSSION

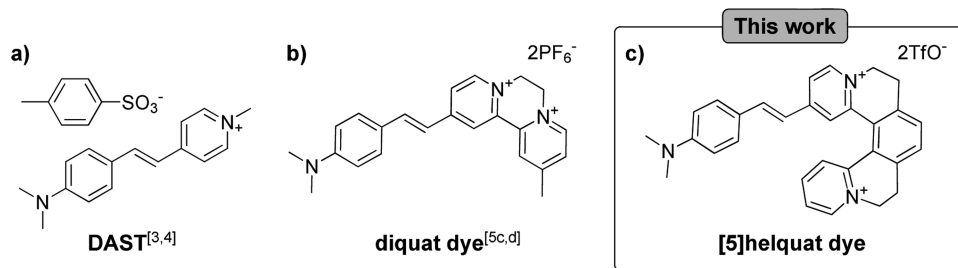
Compounds 1–10 are prepared via Knoevenagel condensations from methyl-substituted [5]helquat or [6]helquat (Scheme 2a and b, respectively). The products are characterized by ¹H/¹³C NMR spectroscopy, elemental analyses, and positive-electro-spray mass spectrometry. Also, two single-crystal X-ray structures have been obtained (Figure 1 and Supporting Information). Although the PF₆[−] analogue of 1 and the triflate salt 6 adopt centrosymmetric structures, this does not preclude significant $\chi^{(2)}$ if β_{xyz} values are substantial. Also, anion metathesis can readily modify crystal packing arrangements.^{10d}

The UV–vis spectra of 1–10 show an intense low energy absorption band attributable to intramolecular charge-transfer (ICT) from the amino unit to the helquat fragment. This behavior is confirmed by DFT and time-dependent DFT (TD-

Received: December 2, 2015

Published: February 4, 2016

Scheme 1. (a) DAST, (b) a Diquat NLO Chromophore, and (c) a Helquat Dye Introduced Here



Scheme 2. Synthesis of (a) [5]Helquat Dyes 1–5 and (b) [6]Helquat Dyes 6–10 via Knoevenagel Condensation Chemistry

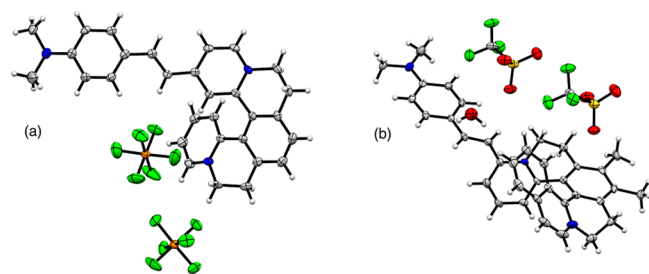
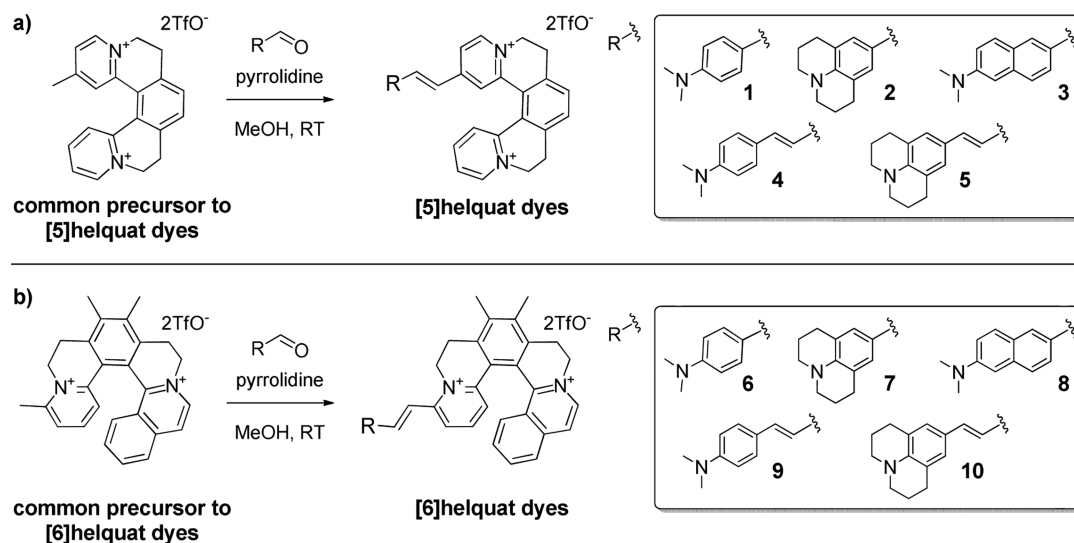


Figure 1. Representations of the molecular structures of (a) the PF_6^- analogue of salt **1** and (b) $6 \cdot \text{H}_2\text{O}$ (50% probability ellipsoids). H = white; C = gray; N = blue; P = orange; F = green; O = red; and S = gold.

DFT) calculations on the cations in salts **1** and **6** (denoted **1'** and **6'**, respectively; details in the [Supporting Information](#)). However, the theoretical λ_{max} values are blue-shifted significantly when compared with the measured values ([Figure 2](#) and [Figure S1](#), [Supporting Information](#)).

The MOs are determined from gas phase calculations, whereas the TD-DFT calculations are carried out using a conductor-like polarizable continuum model (CPCM) of MeCN. Depictions of the frontier MOs and computed transitions are included in the [Supporting Information](#) ([Figures S2 and S3](#), [Table S1](#)). For **1'**, the lowest energy transition has mainly HOMO \rightarrow LUMO character with a small HOMO \rightarrow LUMO+1 contribution. On the other hand, this transition in **6'** has similar contributions from HOMO \rightarrow LUMO and HOMO \rightarrow LUMO+1. In both cations, the HOMO is located on the 4-(dimethylamino)styryl fragment,

whereas the LUMO is based mostly on the helquat unit and the LUMO+1 is spread over the whole molecule ([Figure 3](#)).

The results of 800 nm fs HRS measurements¹¹ of resonant β values and β_0 (derived using the two-state model)¹² for **1–10** in MeCN are shown in [Table 1](#) together with data reported for [DAS]PF₆.¹³ The DFT and TD-DFT results confirm that the new chromophores are described adequately as two-state systems, i.e., a single low energy electronic transition is expected to dominate the NLO response.

Within the [5]helquat series **1–5**, $\beta_0[\text{H}]$ increases in the order **1** \leq **3** \leq **2** $<$ **4** \leq **5**. As for related pseudolinear pyridinium compounds,¹⁴ the stronger π -electron donating ability of the julolidinyl group vs 4-(dimethylamino)phenyl that is evident in the ICT energies E_{max} translates to larger apparent $\beta_0[\text{H}]$ responses for **2** vs **1** and for **5** vs **4**. However, the difference for the latter pair is within the experimental error limits. Also as expected, extending the π -conjugation on moving from **1** to **4** or from **2** to **5** increases $\beta_0[\text{H}]$ significantly. The E_{max} values for **3** and **4** indicate that the electron-donating strength of the aminoaryl unit is weakened when one of the vinyl groups is incorporated into a phenyl ring and $\beta_0[\text{H}]$ thus decreases. The data for [6]helquats **6–10** show the same overall trends with $\beta_0[\text{H}]$ increasing in the order **6** $<$ **8** \leq **7** $<$ **9** \leq **10**. Replacing a [5]helquat with a [6]helquat while also changing the position of attachment of the donor substituent with respect to the quaternized N atom always causes the ICT band to blue shift by ~ 0.1 eV. However, the observed variations in $\beta_0[\text{H}]$ show no clear trend and are in several cases insignificant.

The results of Stark spectroscopic studies¹⁵ on the ICT bands of salts **1–10** in PrCN at 77 K are shown in [Table 1](#) together with

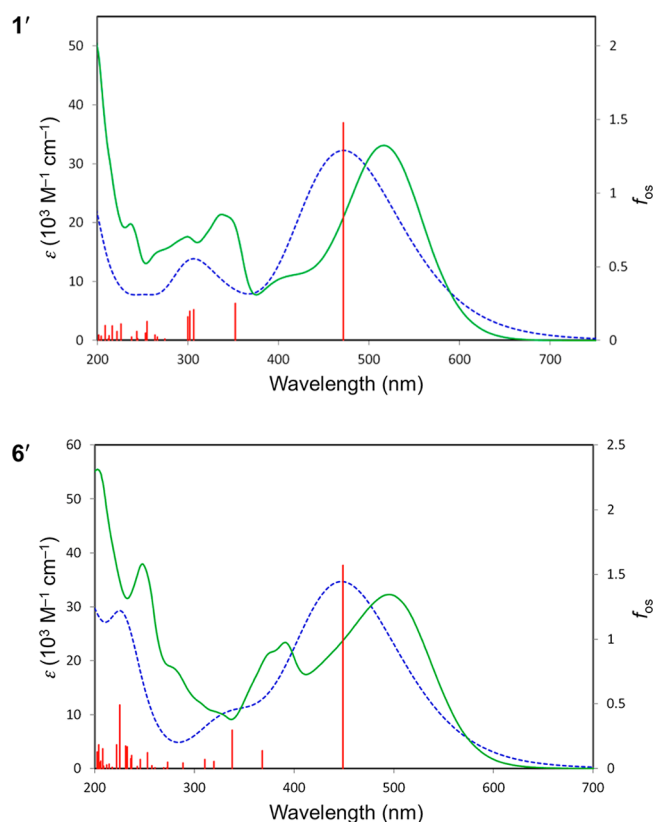


Figure 2. CAM-B3LYP/6-311G(d)-calculated (blue) and experimental (green) UV-vis absorption spectra of **1'** and **6'** in MeCN. The ϵ -axes refer to the experimental data only (for the OTf⁻ salts), and the vertical axes of the calculated data are scaled to match the main experimental absorptions. The f_{0s} -axes refer to the individual calculated transitions (red).

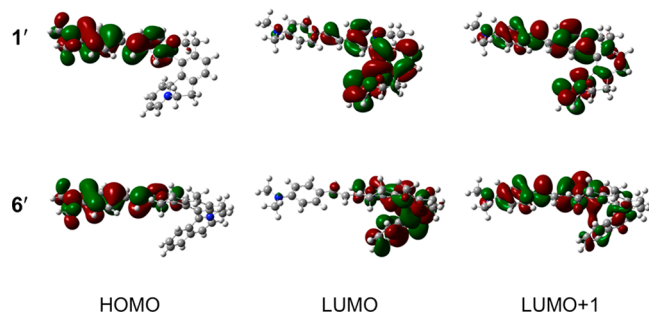


Figure 3. CAM-B3LYP/6-311G(d)-derived contour surface diagrams (gas phase) of the MOs involved in the low energy transitions for cations **1'** (472 nm) and **6'** (449 nm) in a CPCM of MeCN (isosurface value 0.03 au).

data for [DAS]PF₆.¹³ Representative spectra for **2**, **5**, **7**, and **10** are shown in Figure 4. In contrast to the HRS technique that is complicated by resonance effects, the Stark-based approach allows indirect estimation of β_0 values.

For all except **5**, the ICT bands of **1–10** show small red shifts or no significant change on moving from MeCN solutions to PrCN glasses, and the energy ordering within the two series remains constant (Table 1). The decreases in E_{\max} on extending a vinyl to 1,3-butadienyl bridge or replacing a 4-(dimethylamino)-phenyl with julolidinyl group are maintained at 77 K. The μ_{12} values determined using eq 1 all fall into a relatively narrow range with small increases on conjugation extension. In general, $\Delta\mu_{12}$

also increases in the same manner and as expected, although the value for **2** is unexpectedly large whereas that for **9** is low.

For the [5]helquats **1–5**, the β_0 [S] values determined using eq 2 increase in the order $1 \leq 3 \leq 2 \leq 5 \leq 4$, almost paralleling the β_0 [H] data (see above). For the [6]helquats **6–10**, the β_0 [S] ordering of $6 \leq 8 \leq 7 \leq 9 \leq 10$ matches the HRS trend exactly. The expected increases in the NLO response on enhancing the electron donor strength or extending the conjugation are thus also shown by most of the Stark-derived data, except that **4** appears to have a larger β_0 [S] value than **5**. However, the difference is within the estimated error limit of $\pm 20\%$. Also, as for the HRS data, changing the helquat unit leads to variations in β_0 [S] that are generally not statistically significant.

Comparing the β_0 values for **1–10** with those of [DAS]PF₆ reveals that a number of the new dye salts show a similar level of NLO activity and that several compare favorably. In particular, **4**, **5**, **9**, and **10** show β_0 [S] responses twice as large or even greater when compared with this benchmark compound. These enhancements are due to a combination of decreasing E_{\max} and increasing $\Delta\mu_{12}$. These observations provide a strong incentive to pursue further crystalline materials incorporating these new helquat cations in which large bulk NLO effects can be anticipated.

β_0 values calculated via DFT with CAM-B3LYP are shown in Table 2. Such data may be of limited reliability (especially in terms of absolute magnitudes)¹⁶ and should thus be treated with some caution. Nevertheless, neither HRS nor Stark studies give information regarding the contributions of the various tensor components; thus, it is helpful to have some indication of these.

As noted previously for purely organic¹⁶ and ruthenium-based^{16,17} chromophores, β_{tot} increases substantially upon moving from the gas phase to MeCN solution. β_{tot} is also larger for [5]helquat **1'** than for [6]helquat **6'** or for DAS⁺, differences that are reflected only partially in the experimental data (Table 1). With the x -axis aligned approximately with the dipole of the stilbazolium unit (Figure S4), the β_x and β_{xxx} components dominate as expected. The hyperpolarizability of the pseudo-linear DAS⁺ cation is essentially one-dimensional. In contrast, the off-diagonal β_{xxy} components are relatively significant in **1'** but are less important in **6'**. The nondipolar β_{xyz} terms are predicted to be zero for DAS⁺, but still only small in its helquat relatives, which is perhaps disappointing. However, this result can be attributed to the fact that these first-generation helquat units are only partially π -conjugated unlike helicenes. Replacing the quaternizing ethylenes with vinyl linkages will enhance conjugation and give more substantial β_{xyz} responses.

CONCLUSIONS

In summary, we introduce an original class of dicationic helical dyes with strong NLO responses. Notably, both HRS and Stark spectroscopy show that the helquat dye salts **4**, **5**, **9**, and **10** exhibit nonresonant NLO activity significantly higher than [DAS]PF₆. Such activities are more than sufficient for potential applications. DFT confirms that the β_0 values of the cations in **1** and **6** are strongly competitive, but β_{xyz} components are only small due to limited π -conjugation. Helical cationic dyes are therefore a highly attractive platform for developing new systems with substantial NLO responses.

EXPERIMENTAL SECTION

General Methods. Liquids and solutions were transferred via needle and syringe under inert atmosphere unless stated otherwise. *N*-Alkylation reactions and Knoevenagel condensations were run in

Table 1. ICT Absorption, Stark Spectroscopic, and HRS data for Salts 1–10

salt	λ_{\max}^a (nm)	λ_{\max}^b (nm)	E_{\max}^b (eV)	$f_{\text{os}}^{b,c}$	$\mu_{12}^{b,d}$ (D)	$\Delta\mu_{12}^{b,e}$ (D)	$\beta_0[\text{S}]^f$ (10^{-30} esu)	β_{800}^g (10^{-30} esu)	$\beta_0[\text{H}]^h$ (10^{-30} esu)
1	520	526	2.36	0.68	8.7	14.3	258	184 ± 15	73 ± 6
2	570	569	2.18	0.61	8.6	24.2	442	196 ± 7	99 ± 4
3	513	524	2.37	0.66	8.6	20.6	340	235 ± 26	89 ± 10
4	539	549	2.26	0.96	10.6	25.6	658	302 ± 32	135 ± 14
5	600	588	2.11	0.66	9.1	25.9	566	275 ± 26	150 ± 14
6	496	498	2.49	0.56	7.8	22.5	252	171 ± 12	57 ± 4
7	538	537	2.31	0.71	9.0	20.2	364	209 ± 6	93 ± 3
8	485	493	2.52	0.46	7.0	29.5	260	302 ± 13	90 ± 4
9	516	533	2.33	0.82	9.7	21.1	424	401 ± 43	156 ± 17
10	564	564	2.20	0.78	9.7	26.1	588	376 ± 32	187 ± 16
[DAS]PF ₆ ⁱ	470	480	2.58	0.80	9.1	16.3	236	440 ± 30	110 ± 7

^aIn MeCN at 295 K. ^bIn PrCN at 77 K. ^cObtained from $(4.32 \times 10^{-9} \text{ M cm}^2) \epsilon_{\max} \times f_{w_{1/2}}$, where ϵ_{\max} is the maximal molar extinction coefficient and $f_{w_{1/2}}$ is the full width at half height (in wavenumbers). ^dCalculated from eq 1. ^eCalculated from $f_{\text{int}} \Delta\mu_{12}$ using $f_{\text{int}} = 1.33$. ^fCalculated from eq 2. The quoted cgs units (esu) can be converted to SI units ($\text{C}^3 \text{ m}^3 \text{ J}^{-2}$) by dividing by 2.693×10^{20} or into atomic units by dividing by 0.8640×10^{-32} . ^gObtained from HRS measurements with an 800 nm Ti³⁺:sapphire laser and MeCN solutions at 295 K. ^hDerived from β_{800} by application of the two-state model.¹² ⁱData taken from ref 13.

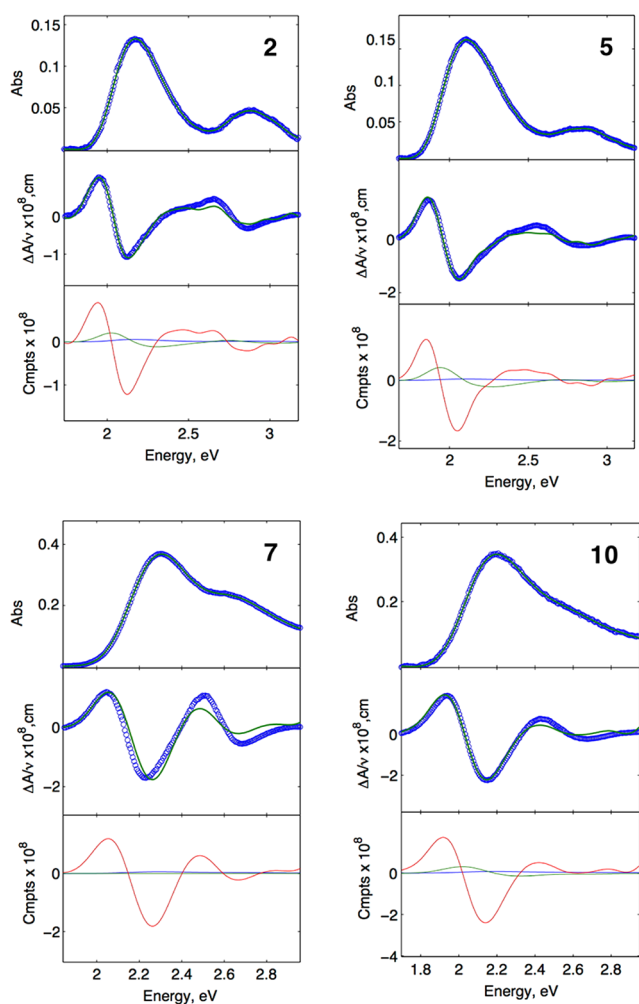


Figure 4. Spectra and calculated fits for salts 2, 5, 7 and 10. Top panel: UV-vis absorption spectrum; middle panel: electroabsorption spectrum, experimental (blue), and fits (green) according to the Liptay equation;^{15b} and bottom panel: contribution of 0th (blue), first (green), and second (red) derivatives of the absorption spectrum to the calculated fits.

vessels covered with Alufoil to prevent prolonged exposure of the organic cations to ambient light. Melting points were determined on a

micro-melting point apparatus and are uncorrected. Thin-layer chromatography (TLC) analysis was performed on silica gel plates (Silica gel 60 F₂₅₄-coated aluminum sheets) and visualized by UV (UV lamp 254/365 nm) and/or chemical staining with KMnO₄ [KMnO₄ (1% aq), Na₂CO₃ (2% aq)]. TLC analysis of dications was achieved using Stoddart's magic mixture¹⁸ (MeOH/NH₄Cl aq (2M)/MeNO₂ 7:2:1) as eluent on silica gel plates. NMR spectra were measured at 600 MHz for ¹H and 151 MHz for ¹³C or at 400 MHz for ¹H and 101 MHz for ¹³C. In ¹H and ¹³C NMR spectra, chemical shifts are referenced as follows (ppm): in acetone-*d*₆, the peaks were referenced relative to the solvent peak $\delta_{\text{H}} = 2.09$ ppm and $\delta_{\text{C}} = 29.80$ ppm and in acetonitrile-*d*₃ relative to the solvent peak $\delta_{\text{H}} = 1.94$ ppm and $\delta_{\text{C}} = 118.26$ ppm. Chemical shifts are given in δ -scale as parts per million (ppm); coupling constants (*J*) are given in Hertz. High-resolution mass spectra (HRMS) were obtained with a hybrid FT mass spectrometer using electrospray (+ mode) ionization technique and linear ion trap MS in combination with the orbitrap mass analyzer. The mobile phase consisted of MeOH/water (9:1) with a flow rate of 200 $\mu\text{L min}^{-1}$. The sample was dissolved, diluted with the mobile phase, and injected using a 5 μL loop. Spray voltage, capillary voltage, tube lens voltage, and capillary temperature were 5.5 kV, 5 V, 80 V, and 275 $^{\circ}\text{C}$, respectively. High-resolution mass spectra (HRMS) were obtained with the ESI instrument. Dichloromethane (DCM) and triethylamine were purified via distillation under argon over CaH₂ and were used directly after distillation. MeOH was distilled from Mg/I₂ as follows. MeOH (100 mL) was charged into a 1 L round-bottomed flask. Then, 5 g of Mg was added followed by addition of I₂ (500 mg). The mixture was heated to reflux under Ar atmosphere for 15 min. Then, more I₂ (500 mg) and MeOH (500 mL) were added, and the mixture was refluxed under Ar atmosphere for 2 h. MeOH was then stored under Ar atmosphere over 4 Å activated molecular sieves. Degassed solvents were obtained via the freeze-pump-thaw method. The solvent was frozen under argon and then thawed under vacuum. This process was repeated three times. Finally, the thawed solvent was purged with argon. Unless otherwise stated, all other starting materials and reagents were obtained from commercial suppliers and used without further purification.

Synthesis of [5]Helquat Dyes 1–5. (*E*)-2-(4-(Dimethylamino)styryl)-6,7,10,11-tetrahydropyrido[2,1-*a*:1',2'-*k*][2,9]-phenanthroline-5,12-dium Trifluoromethanesulfonate (1). Methyl-substituted [5]helquat (87 mg, 0.145 mmol) and the aldehyde (43 mg, 0.288 mmol, 2.0 equiv) were placed in a Schlenk flask under an argon atmosphere. MeOH (2 mL) was added, and the solids were dissolved while stirring. Then, the flask was covered with Alufoil, and pyrrolidine (115 μL , 100 mg, 1.400 mmol, 9.7 equiv) was added at once. The mixture was stirred at RT for 2 h until disappearance of the starting helquat was detected. The reaction was quenched with Et₂O (20 mL), causing precipitation. The suspension was centrifuged, and the supernatant was separated. The solid residue was then dissolved in

Table 2. Static First Hyperpolarizabilities (10^{-30} esu) Calculated at the CAM-B3LYP/6-311G(d) Level for the Cations **1'**, **6'**, and DAS⁺

cation	β_{xxx}	β_{xyx}	β_{yxy}	β_{yyy}	β_{xxz}	β_{xyz}	β_{yyz}	β_{zzz}	β_{zzx}	β_{yzz}	β_{zxx}	β_x	β_y	β_z	β_{tot}
1'^a	235.6	-45.7	9.7	3.9	29.6	-1.5	2.2	1.3	1.8	1.2	246.6	-39.9	32.9	252	
1'^b	582.9	-180.4	32.5	2.4	72.3	-11.3	4.1	0.6	2.8	2.1	616.1	-175.2	78.5	645	
6'^a	-206.6	-11.8	-1.7	-9.3	29.4	-1.6	-0.3	-3.1	0.5	0.0	-211.4	-20.7	29.2	214	
6'^b	-451.3	-21.8	-0.5	-22.7	86.3	-3.4	0.6	-9.8	1.5	0.6	-461.6	-43.0	87.5	472	
DAS ^{+a}	-193.0	-5.7	5.2	-0.1	0.3	0.0	-0.1	0.2	0.0	0.1	-187.6	-5.9	0.3	188	
DAS ^{+b}	-511.3	-8.7	13.8	-0.9	0.5	0.0	-0.2	0.6	-0.1	0.2	-496.9	-9.7	0.5	497	

^aIn the gas phase. ^bIn MeCN.

MeOH (1 mL), and the product was precipitated by the addition of Et₂O (10 mL). The resulting suspension was centrifuged, and the supernatant was separated. The resulting solid was dissolved in MeOH (1 mL), and the precipitation procedure was repeated (with 10 mL of Et₂O). Finally, the solid was separated and dried in a vacuum, giving pure [5]helquat dye **1** as a dark violet solid. Mp: 177–179 °C. Yield: 97 mg, 92%. ¹H NMR (400 MHz, CD₃CN): δ 3.03 (s, 6H), 3.21–3.38 (m, 4H), 4.54–4.98 (m, 4H), 6.74 (d, J = 9.0 Hz, 2H), 6.83 (d, J = 16.0 Hz, 1H), 7.38–7.47 (m, 3H), 7.67 (d, J = 1.9 Hz, 1H), 7.70 (s, 2H), 7.80 (dd, J = 2.0, 6.7 Hz, 1H), 7.87–7.92 (m, 1H), 8.03–8.07 (m, 1H), 8.15–8.21 (m, 1H), 8.46 (d, J = 6.8 Hz, 1H), 8.81–8.85 (m, 1H). ¹³C NMR (100 MHz, CD₃CN): δ 28.2, 28.8, 40.4, 54.5, 56.3, 113.1, 117.6, 121.1, 121.3, 123.3, 123.5, 126.3, 127.0, 127.5, 127.9, 131.0, 131.4, 133.2, 133.7, 141.6, 143.8, 145.4, 145.7, 146.5, 147.0, 148.3, 153.7, 155.5. Elemental analysis: (%) calcd for [C₃₂H₂₉F₆N₃O₆S₂] C 52.67, H 4.01, N 5.76; found C 52.20, H 3.90, N 5.59. IR (neat): $\tilde{\nu}$ 3091, 1640, 1580, 1513, 1442, 1262, 1229, 1165, 1033, 640, 519. MS (ESI): m/z (%) 580 (59), 430 (100). HRMS (ESI): m/z calcd for [(M – TfO⁻)⁺] (C₃₁H₂₉F₆N₃O₆S) 580.1876; found 580.1873.

(*E*)-2-(2-(2,3,6,7-Tetrahydro-1*H*,5*H*-pyrido[3,2,1-*ij*]quinolin-9-yl)-vinyl)-6,7,10,11-tetrahydrodipyrido[2,1-*a*:1',2'-*k*][2,9]phenanthroline-5,12-dium Trifluoromethanesulfonate (**2**). This compound was prepared and purified in a manner similar to dye **1** using methyl-substituted [5]helquat (50 mg, 0.084 mmol), 9-julolidine carboxaldehyde (34 mg, 0.169 mmol, 2.0 equiv), MeOH (4 mL), and pyrrolidine (84 μ L, 73 mg, 1.022 mmol, 12.0 equiv). Precipitation was performed with Et₂O (40 mL). Reprecipitation was performed twice using MeOH (1 mL) and addition of Et₂O (10 mL) to form a dark blue solid. Mp: 195–197 °C. Yield: 60 mg, 92%. ¹H NMR (400 MHz, CD₃CN): δ 1.86–1.94 (m, 4H), 2.69 (t, J = 6.3 Hz, 4H), 3.21–3.34 (m, 8H), 4.49–4.97 (m, 4H), 6.69 (d, J = 15.9 Hz, 1H), 6.99 (s, 2H), 7.29 (d, J = 15.9 Hz, 1H), 7.56 (d, J = 2.0 Hz, 1H), 7.68–7.71 (m, 3H), 7.86–7.92 (m, 1H), 8.02–8.06 (m, 1H), 8.14–8.20 (m, 1H), 8.36 (d, J = 6.8 Hz, 1H), 8.80 (m, 1H). ¹³C NMR (100 MHz, CD₃CN): δ 22.2, 28.2, 28.4, 28.9, 50.7, 54.2, 56.3, 116.1, 120.5, 121.1, 122.4, 122.5, 123.2, 126.0, 126.9, 127.4, 128.0, 129.3, 131.0, 133.0, 133.7, 141.5, 144.3, 145.0, 145.5, 146.1, 147.0, 147.1, 148.4, 155.4. Elemental analysis: (%) calcd for [C₃₆H₃₃F₆N₃O₆S₂] C 55.31, H 4.25, N 5.37; found C 54.83, H 4.14, N 5.05. IR (neat): $\tilde{\nu}$ 3095, 1638, 1571, 1513, 1472, 1261, 1227, 1211, 1154, 1032, 639, 575. MS (ESI): m/z (%) 632 (26), 241 (100). HRMS (ESI): m/z calcd for [(M – TfO⁻)⁺] (C₃₅H₃₃F₆N₃O₆S) 632.2189; found 632.2188.

(*E*)-2-(2-(6-(Dimethylamino)naphthalen-2-yl)vinyl)-6,7,10,11-tetrahydrodipyrido[2,1-*a*:1',2'-*k*][2,9]phenanthroline-5,12-dium Trifluoromethanesulfonate (**3**). This compound was prepared and purified in a manner similar to dye **1** using methyl-substituted [5]helquat (100 mg, 0.167 mmol), 6-dimethylaminonaphthalaldehyde (70 mg, 0.351 mmol, 2.1 equiv), MeOH (10 mL), and pyrrolidine (168 μ L, 146 mg, 2.045 mmol, 12.3 equiv). Precipitation was performed with Et₂O (50 mL). Reprecipitation was performed twice using MeOH (10 mL) and the addition of Et₂O (50 mL) to form a dark violet solid. Mp: 212–214 °C. Yield: 118 mg, 90%. ¹H NMR (400 MHz, CD₃CN): δ 3.08 (s, 6H), 3.24–3.36 (m, 4H), 4.59–5.00 (m, 4H), 6.95 (d, J = 2.5 Hz, 1H), 7.10 (d, J = 16.2 Hz, 1H), 7.23 (dd, J = 2.6, 9.1 Hz, 1H), 7.54–7.62 (m, 2H), 7.64 (d, J = 7.6 Hz, 1H), 7.72 (s, 2H), 7.76 (d, J = 9.2 Hz, 1H), 7.80–7.83 (m, 2H), 7.89–7.95 (m, 2H), 8.03–8.07 (m, 1H), 8.16–8.22 (m, 1H), 8.57 (d, J = 6.7 Hz, 1H), 8.84–8.88 (m, 1H). ¹³C NMR (100

MHz, CD₃CN): δ 28.2, 28.6, 40.7, 54.8, 56.3, 106.6, 117.6, 121.1, 121.2, 122.2, 124.7, 126.9, 127.0, 127.6, 127.7, 128.0, 129.4, 130.9, 131.0, 131.9, 133.4, 133.8, 137.7, 141.7, 143.5, 145.8, 145.8, 147.0, 147.1, 148.2, 151.3, 155.1. Elemental analysis: (%) calcd for [C₃₆H₃₁F₆N₃O₆S₂·H₂O] C 54.20, H 4.17, N 5.27; found C 54.42, H 4.47, N 5.31. IR (neat): $\tilde{\nu}$ 3098, 1637, 1594, 1513, 1438, 1262, 1228, 1166, 1127, 1033, 639, 576, 520. MS (ESI): m/z (%) 630 (38), 240 (100). HRMS (ESI): m/z calcd for [(M – TfO⁻)⁺] (C₃₅H₃₁F₆N₃O₆S) 630.2033; found 630.2032.

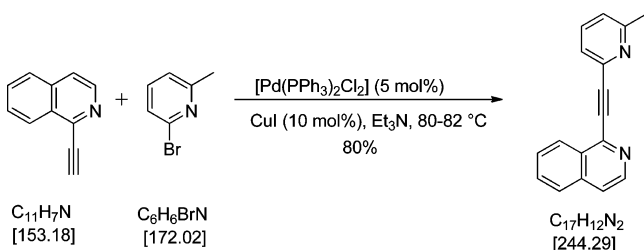
2-((1*E*,3*E*)-4-(4-(Dimethylamino)phenyl)buta-1,3-dien-1-yl)-6,7,10,11-tetrahydrodipyrido[2,1-*a*:1',2'-*k*][2,9]phenanthroline-5,12-dium Trifluoromethanesulfonate (**4**). This compound was prepared and purified in a manner similar to dye **1** using methyl-substituted [5]helquat (134 mg, 0.224 mmol), (*E*)-3-(4-(dimethylamino)phenyl)acrylaldehyde (78 mg, 0.445 mmol, 2.0 equiv), MeOH (2 mL), and pyrrolidine (224 μ L, 194 mg, 2.728 mmol, 12.2 equiv). Precipitation was performed with Et₂O (20 mL). Reprecipitation was performed twice using MeOH (2 mL) and the addition of Et₂O (20 mL) to form a dark blue solid. Mp: 205–207 °C. Yield: 109 mg, 65%. ¹H NMR (400 MHz, CD₃CN): δ 3.00 (s, 6H), 3.19–3.38 (m, 4H), 4.52–4.98 (m, 4H), 6.41 (d, J = 15.3 Hz, 1H), 6.70–6.75 (m, 2H), 6.80–6.95 (m, 2H), 7.32 (dd, J = 10.3, 15.3 Hz, 1H), 7.40–7.45 (m, 2H), 7.62 (d, J = 1.9 Hz, 1H), 7.71 (s, 2H), 7.76 (dd, J = 2.0, 6.7 Hz, 1H), 7.88–7.93 (m, 1H), 8.00–8.04 (m, 1H), 8.18 (td, J = 8.1, 1.4 Hz, 1H), 8.46 (d, J = 6.7 Hz, 1H), 8.81–8.85 (m, 1H). ¹³C NMR (100 MHz, CD₃CN): δ 28.2, 28.7, 40.4, 54.6, 56.2, 113.1, 121.1, 121.8, 123.3, 123.6, 123.7, 124.7, 126.4, 126.9, 127.6, 127.8, 130.4, 131.0, 133.3, 133.8, 141.6, 141.6, 144.4, 145.1, 145.5, 145.7, 146.6, 147.0, 148.2, 152.9, 155.0. Elemental analysis: (%) calcd for [C₃₄H₃₁F₆N₃O₆S₂] C 54.03, H 4.13, N 5.56; found: C 54.10, H 4.11, N 5.51. IR (neat): $\tilde{\nu}$ 3094, 1639, 1572, 1515, 1441, 1371, 1279, 1262, 1229, 1151, 1033, 1005, 759, 640, 576. MS (ESI): m/z (%) 606 (14), 228 (100). HRMS (ESI): m/z calcd for [(M – TfO⁻)⁺] (C₃₃H₃₁F₆N₃O₆S) 606.2033; found 606.2034.

(*E*)-3-(1,2,3,5,6,7-Hexahydropyrido[3,2,1-*ij*]quinolin-9-yl)-acrylaldehyde (**11**).¹⁴ A previously published procedure¹⁴ was followed with some modifications: 9-julolidine carboxaldehyde (500 mg, 2.484 mmol, 1.0 equiv), ((1,3-dioxolan-2-yl)methyl)tributylphosphonium bromide (4.587 g, 12.42 mmol, 5.0 equiv), NaH (60% in mineral oil, 400 mg, 10 mmol, 4.0 equiv), and 18-crown-6 (33 mg, 0.124 mmol, 5 mol %) were charged into an oven-dried Schlenk flask and placed under argon using a vacuum/argon manifold. Under an argon atmosphere, THF (20 mL) was added. The mixture was stirred at RT for 2.5 h. After disappearance of 9-julolidine carboxaldehyde was detected (TLC), water (20 mL) was added, and the resulting mixture was extracted with Et₂O (3 \times 20 mL). The combined organic layers were dried over MgSO₄ and filtered through a Celite pad. The Celite pad was washed with Et₂O (3 \times 5 mL). Volatiles from the filtrate were removed on a rotary evaporator, and the crude residue was mixed with THF/10% HCl (1.5:1, 10 mL) and stirred at RT for 0.5 h until complete consumption of the acetal. The reaction mixture was quenched by the addition of water (20 mL), and the resulting solution was extracted with Et₂O (3 \times 25 mL). The combined ethereal extracts were dried over Na₂SO₄ and then filtered through a Celite pad. The solid residue after removal of the volatiles was washed with pentane (10 mL), and the resulting aldehyde was dried in a vacuum. Mp: 125–127 °C. Yield: 422 mg, 75%. ¹H NMR (400 MHz, acetone-*d*₆): δ 1.92–1.99 (m, 4H), 2.73–2.78 (m, 4H), 3.29–3.33 (m, 4H), 6.46 (dd, J = 7.8, 15.5 Hz, 1H), 7.11 (m, 2H), 7.40 (d, J = 15.5 Hz, 1H), 9.56 (d, J = 7.8 Hz, 1H). ¹³C NMR (100 MHz,

acetone- d_6): δ 22.2, 28.2, 50.4, 121.7, 121.8, 123.4, 128.9, 146.4, 154.8, 193.2. IR (KBr): $\tilde{\nu}$ 837, 1126, 1318, 1451, 1523, 1639, 1654, 3166, 3279. MS (ESI): m/z (%) 228.1 (100), 250.1 (35), 477.2 (15). HRMS (ESI): m/z calcd for (C₁₅H₁₈ON) 228.1383; found 228.1381.

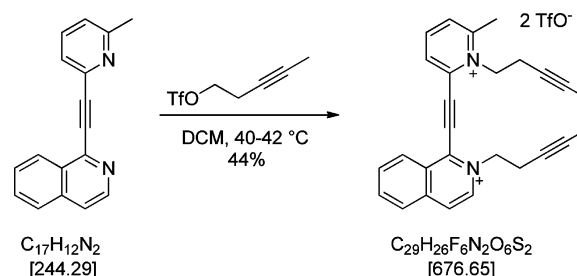
2-((1*E*,3*E*)-4-(2,3,6,7-Tetrahydro-1*H*,5*H*-pyrido[3,2-*i*]quinolin-9-yl)buta-1,3-dien-1-yl)-6,7,10,11-tetrahydridiprido[2,1-*a*:1',2'-*k*]-[2,9]phenanthroline-5,12-dium Trifluoromethanesulfonate (5). This compound was prepared and purified in a manner similar to dye 1 using methyl-substituted [5]helquat (43 mg, 0.072 mmol), (*E*)-3-(1,2,3,5,6,7-hexahydropyrido[3,2,1-*i*]quinolin-9-yl)acrylaldehyde (33 mg, 0.145 mmol, 2.0 equiv), MeOH (4 mL), and pyrrolidine (72 μ L, 62 mg, 0.876 mmol, 12.2 equiv). Precipitation was performed with Et₂O (40 mL). Reprecipitation was performed twice using MeOH (4 mL) to form a dark blue solid. Mp: 225–227 °C. Yield: 41 mg, 70%. ¹H NMR (400 MHz, CD₃CN): δ 1.86–1.96 (m, 4H), 2.69 (t, *J* = 6.3 Hz, 4H), 3.21–3.34 (m, 8H), 4.49–4.98 (m, 4H), 6.33 (d, *J* = 15.2 Hz, 1H), 6.70–6.84 (m, 2H), 6.98 (s, 2H), 7.29 (dd, *J* = 10.0, 15.2 Hz, 1H), 7.55 (d, *J* = 1.9 Hz, 1H), 7.68–7.74 (m, 3H), 7.87–7.92 (m, 1H), 8.00–8.04 (m, 1H), 8.15–8.21 (m, 1H), 8.40 (d, *J* = 6.8 Hz, 1H), 8.80–8.84 (m, 1H). ¹³C NMR (100 MHz, CD₃CN): δ 22.4, 28.2, 28.4, 28.8, 50.7, 54.4, 56.3, 121.1, 121.3, 122.4, 122.6, 122.7, 123.3, 123.7, 126.1, 126.9, 127.5, 127.9, 128.3, 131.0, 133.1, 133.7, 141.5, 141.5, 145.2, 145.3, 145.5, 145.6, 146.0, 146.4, 147.0, 148.3, 155.0. Elemental analysis: (%) calcd for [C₃₈H₃₅F₆N₃O₆S₂] C 56.50, H 4.37, N 5.20; found C 56.50, H 4.21, N 4.99. IR (neat): $\tilde{\nu}$ 3086, 1624, 1563, 1511, 1483, 1269, 1262, 1225, 1209, 1146, 1032, 1029, 756, 640, 573. MS (ESI): m/z (%) 658 (4), 254 (100). HRMS (ESI): m/z calcd for [(M – TfO[−])⁺] (C₃₇H₃₅F₃N₃O₃S) 658.2346; found 658.2347.

Synthesis of [6]Helquat Dye Precursor. 1-((6-Methylpyridin-2-yl)ethynyl)isoquinoline (12). [Pd(PPh₃)₂Cl₂] (1.150 g, 1.638 mmol, 5



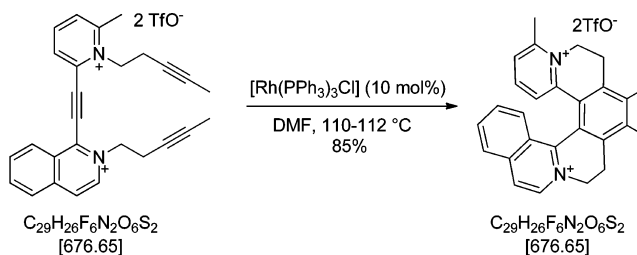
mol %), CuI (0.622 g, 3.266 mmol, 10 mol %), and 1-ethynylisoquinoline (5.000 g, 32.64 mmol, 1.0 equiv) were placed under argon in an oven-dried Schlenk flask. Under an argon atmosphere, triethylamine (200 mL) was added followed by 2-bromo-6-methylpyridine (6.737 g, 39.16 mmol, 1.2 equiv). The mixture was stirred under argon while heating at 80–82 °C for 1 h, which is when the disappearance of 1-ethynylisoquinoline was detected. The reaction mixture was allowed to cool to RT and filtered through a Celite pad. The Celite pad was repeatedly washed with EtOAc until no product was detected in the eluent (TLC analysis). The volatiles from the filtrate were removed using a rotary evaporator, and the crude residue was purified by column chromatography on silica gel using hexane/EtOAc (50:50) as eluent to form a brownish solid. Mp: 113–116 °C. Yield: 6.370 g, 80%. ¹H NMR (600 MHz, (CD₃)₂CO): δ 2.61 (s, 3H), 7.39 (d, *J* = 7.8 Hz, 1H), 7.69 (d, *J* = 7.6 Hz, 1H), 7.83 (t, *J* = 7.7 Hz, 1H), 7.86 (ddd, *J* = 1.2, 6.7, 8.2 Hz, 1H), 7.89 (ddd, *J* = 1.4, 6.7, 8.3 Hz, 1H), 7.92 (dd, *J* = 1.3, 5.6 Hz, 1H), 8.08 (ddt, *J* = 0.8, 1.3, 8.3 Hz, 1H), 8.62 (ddd, *J* = 0.8, 1.4, 8.2 Hz, 1H), 8.63 (d, *J* = 5.6 Hz, 1H). ¹³C NMR (151 MHz, (CD₃)₂CO): δ 24.5, 85.8, 93.5, 122.0, 124.4, 125.8, 127.2, 128.1, 129.4, 130.3, 131.7, 136.7, 142.6, 144.0, 144.2, 160.2. IR (KBr): $\tilde{\nu}$ 1495, 1552, 1566, 1581, 1619, 2212, 3009, 3054. MS (ESI): m/z (%) 245.1 (100), 246.1 (20), 267.1 (10). HRMS (ESI): m/z calcd for (C₁₇H₁₃N₂) 245.1073; found 245.1072.

1-((6-Methyl-1-(pent-3-yn-1-yl)pyridin-1-ium-2-yl)ethynyl)-2-(pent-3-yn-1-yl)isoquinolin-2-ium Trifluoromethanesulfonate (13). 1-((6-Methylpyridin-2-yl)ethynyl)isoquinoline (12, 1.000 g, 4.093 mmol, 1.0 equiv) was charged into an oven-dried Carius tube and put under argon. Under an argon atmosphere, dichloromethane (40 mL) was added followed by pent-3-yn-1-yl trifluoromethanesulfonate^{10d}



(4.450 g, 20.586 mmol, 5.0 equiv). The mixture was protected from ambient light with Alufoil cover and stirred at 40–42 °C for 62 h. The reaction mixture was allowed to cool to RT and then transferred to a round bottomed flask for removal of the volatiles on a rotary evaporator. The residue was washed with Et₂O (20 mL) using sonication. The supernatant was separated after centrifugation. This washing, sonication, and supernatant removal was repeated two more times (2 × 20 mL Et₂O). The resulting solid was extracted using dichloromethane (25 mL) and water (40 mL). The emulsion was sonicated vigorously and then centrifuged. After centrifugation, the dichloromethane layer was taken and washed with water twice (2 × 40 mL). The combined aqueous layers were washed with dichloromethane (2 × 35 mL). The oily residue after complete evaporation of water from the aqueous layer (rotary evaporator) was triturated with Et₂O (sonication, 2 × 25 mL) to give a solid. After drying in vacuum, the pure triyne product was obtained as a brownish solid. Mp: 151–154 °C. Yield: 1.23 g, 44%. ¹H NMR (600 MHz, (CD₃)₂CO): δ 1.74 (t, *J* = 2.6 Hz, 3H), 1.77 (t, *J* = 2.6 Hz, 3H), 3.27–3.30 (m, 4H), 3.31 (s, 3H), 5.44 (t, *J* = 6.6 Hz, 2H), 5.50 (t, *J* = 6.6 Hz, 2H), 8.33 (ddd, *J* = 1.2, 7.0, 8.5 Hz, 1H), 8.46 (ddd, *J* = 1.1, 7.0, 8.4 Hz, 1H), 8.46 (dd, *J* = 1.6, 7.9 Hz, 1H), 8.59 (dt, *J* = 1.2, 8.4 Hz, 1H), 8.81 (t, *J* = 7.9 Hz, 1H), 8.90 (dd, *J* = 1.6, 7.9 Hz, 1H), 8.93 (dd, *J* = 0.8, 6.8 Hz, 1H), 9.09 (dq, *J* = 1.0, 8.5 Hz, 1H), 9.20 (d, *J* = 6.8 Hz, 1H). ¹³C NMR (151 MHz, (CD₃)₂CO): δ 3.2, 3.2, 20.0, 21.8, 22.0, 56.5, 61.2, 74.2, 74.3, 82.0, 82.2, 90.1, 99.4, 128.6, 129.3, 130.0, 131.0, 133.6, 134.1, 134.4, 136.3, 138.5, 138.5, 138.6, 138.9, 146.3, 160.7. IR (KBr): $\tilde{\nu}$ 518, 574, 639, 1031, 1172, 1265, 1491, 1509, 1564, 1581, 1602, 1611, 1619, 2223, 2291, 3092. MS (ESI): m/z (%) 295.1 (4), 296.1 (15), 311.1 (36), 312.1 (10), 377.2 (100), 378.2 (31), 395.2 (13), 527.1 (11). HRMS (ESI): m/z calcd for (C₂₈H₂₆O₃N₂F₃S) 527.1611; found 527.1612.

[6]Helquat Dye Precursor: 6,7,11-Trimethyl-4,5,8,9-tetrahydroisoquinolino[1,2-*a*]pyrido[1,2-*k*][2,9]phenanthroline-



3,10-dium Trifluoromethanesulfonate (14). [Rh(PPh₃)₃Cl] (0.264 g, 0.285 mmol, 10 mol %) and the dicationic triyne 13 (1.927 g, 2.848 mmol, 1.0 equiv) were charged into an oven-dried Schlenk flask and placed under argon. Under an argon atmosphere, dry and degassed DMF (250 mL) was added. The mixture was stirred at 110–112 °C for 1 h while being protected from ambient light with Alufoil. After complete disappearance of starting material was detected (TLC-mobile phase: Stoddart's magic mixture¹⁸ = MeOH/NH₄Cl aq (2M)/MeNO₂ 7:2:1), the reaction mixture was allowed to cool to RT and then transferred to a round bottomed flask to remove the solvent on a rotary evaporator. The residue was sonicated with THF (25 mL), and the resulting suspension was transferred to centrifuge tubes. The supernatants were separated after centrifugation. The resulting solid was triturated two more times with THF (sonication, 2 × 25 mL), and finally, the solid was triturated three times with Et₂O (3 × 20 mL). The resulting solid was dried in a vacuum to give pure [6]helquat dye precursor as a light yellow solid. Mp: 241–243 °C. Yield: 1.630 g, 85%. ¹H NMR (600 MHz, (CD₃)₂CO): δ

2.66 (s, 6H), 3.16 (s, 3H), 3.38 (dt, $J = 4.8, 15.7$ Hz, 1H), 3.48 (dt, $J = 4.5, 15.3$ Hz, 1H), 3.81 (ddd, $J = 1.7, 3.6, 17.0$ Hz, 1H), 3.83 (ddd, $J = 1.9, 3.7, 17.0$ Hz, 1H), 5.10 (dt, $J = 3.7, 14.4$ Hz, 1H), 5.17 (dt, $J = 3.6, 14.0$ Hz, 1H), 5.39 (ddd, $J = 1.7, 4.5, 14.0$ Hz, 1H), 5.59 (ddd, $J = 1.9, 4.8, 14.2$ Hz, 1H), 7.48 (dd, $J = 2.7, 6.8$ Hz, 1H), 7.74 (t, $J = 7.4$ Hz, 1H), 7.76 (dd, $J = 2.7, 7.8$ Hz, 1H), 7.83 (ddd, $J = 1.2, 6.9, 8.7$ Hz, 1H), 7.99 (ddd, $J = 1.1, 6.9, 8.1$ Hz, 1H), 8.09 (dq, $J = 0.8, 8.7$ Hz, 1H), 8.29 (d, $J = 8.1$ Hz, 1H), 8.55 (d, $J = 6.7$ Hz, 1H), 9.03 (d, $J = 6.7$ Hz, 1H). ^{13}C NMR (151 MHz, $(\text{CD}_3)_2\text{CO}$): δ 16.8, 17.0, 21.4, 26.0, 26.9, 50.2, 56.2, 123.8, 125.9, 127.0, 128.7, 128.8, 128.9, 129.2, 129.2, 132.8, 136.2, 137.6, 138.9, 140.0, 141.1, 142.0, 142.6, 144.4, 148.9, 151.7, 157.0. Elemental analysis: (%) calcd for $[\text{C}_{29}\text{H}_{26}\text{F}_6\text{N}_3\text{O}_6\text{S}_2]$ C 51.48, H 3.87, N 4.14; found C 51.07, H 3.95, N 4.00. IR (KBr): $\tilde{\nu}$ 518, 638, 1031, 1154, 1265, 1491, 1509, 1564, 1581, 1602, 1611, 1619, 3080. MS (ESI): m/z (%) 181.6 (4), 377.2 (100), 378.2 (34), 527.2 (4). HRMS (ESI): m/z calcd for $[(\text{M} - \text{CF}_3\text{SO}_3^-)^+]$ ($\text{C}_{28}\text{H}_{26}\text{F}_3\text{N}_2\text{O}_3\text{S}$) 527.1611; found 527.1612.

Synthesis of [6]Helquat Dyes 6–10. (*E*)-11-(4-(Dimethylamino)styryl)-6,7-dimethyl-4,5,8,9-tetrahydroisoquinolino[1,2-*a*]pyrido[1,2-*k*][2,9]phenanthroline-3,10-dium Trifluoromethanesulfonate (**6**). [6]Helquat dye precursor **14** (70 mg, 0.103 mmol, 1.0 equiv) and 4-dimethylaminobenzaldehyde (47 mg, 0.315 mmol, 3.1 equiv) were charged into a Schlenk flask and placed under argon. Dry MeOH (7.0 mL) was added to the reaction mixture followed by pyrrolidine (100 μL , 87 mg, 1.217 mmol, 11.8 equiv). The flask was covered with Alufoil, and the reaction mixture was stirred at RT for 1 h. The progress of the reaction was monitored by TLC (Stoddart's magic mixture, starting helquat $R_f = 0.5$, product $R_f = 0.75$). The reaction was quenched by the addition of Et_2O (24 mL) and a purple colored solid precipitated. The suspension was sonicated for 2 min and then centrifuged. The supernatant was separated from the solid. The solid was further purified by dissolution in MeOH (2 mL) and precipitated by adding Et_2O (16 mL). The suspension was sonicated and centrifuged, and the supernatant was separated. This dissolution precipitation procedure was repeated two more times. After drying in a vacuum, [6]helquat dye **6** was obtained as a purple solid. Mp: >350 °C. Yield: 56 mg (67%). ^1H NMR (600 MHz, $(\text{CD}_3)_2\text{CO}$): δ 2.66 (s, 3H), 2.66 (s, 3H), 3.15 (s, 6H), 3.34 (ddd, $J = 4.2, 14.4, 17.3$ Hz, 1H), 3.48 (dt, $J = 4.0, 16.2$ Hz, 1H), 3.82 (dt, $J = 3.7, 16.8$ Hz, 1H), 3.82 (dt, $J = 3.5, 16.8$ Hz, 1H), 5.12 (dt, $J = 3.7, 14.2$ Hz, 1H), 5.17 (dt, $J = 3.5, 14.7$ Hz, 1H), 5.40 (dd, $J = 4.0, 13.5$ Hz, 1H), 5.68 (ddd, $J = 1.6, 4.2, 13.3$ Hz, 1H), 6.87–6.90 (m, 2H), 7.3 (d, $J = 8.0$ Hz, 1H), 7.63 (t, $J = 8.1$ Hz, 1H), 7.68 (d, $J = 15.6$ Hz, 1H), 7.77–7.80 (m, 2H), 7.82 (d, $J = 15.6$ Hz, 1H), 7.84 (ddd, $J = 1.2, 7.0, 8.5$ Hz, 1H), 7.99 (dd, $J = 7.0, 8.2$ Hz, 1H), 8.07 (d, $J = 8.2$ Hz, 1H), 8.13 (d, $J = 8.5$ Hz, 1H), 8.29 (d, $J = 8.2$ Hz, 1H), 8.55 (d, $J = 6.7$ Hz, 1H), 9.04 (d, $J = 6.7$ Hz, 1H). ^{13}C NMR (151 MHz, $(\text{CD}_3)_2\text{CO}$): δ 16.8, 16.9, 26.2, 26.8, 40.1, 49.9, 56.2, 111.9, 112.8, 123.4, 123.6, 124.3, 125.7, 126.9, 127.6, 128.8, 129.1, 129.2, 131.8, 132.6, 136.1, 137.4, 138.6, 139.8, 140.5, 141.7, 142.3, 142.5, 146.5, 147.6, 151.9, 153.7, 155.9. Elemental analysis: (%) calcd for $[\text{C}_{38}\text{H}_{35}\text{F}_6\text{N}_3\text{O}_6\text{S}_2 \cdot 0.5\text{H}_2\text{O}]$ C 55.88, H 4.44, N 5.14; found C 55.75, H 4.35, N 5.20. IR (KBr): $\tilde{\nu}$ 3076, 1591, 1555, 1530, 1269, 1164, 1030, 638, 573, 517. MS (ESI): m/z (%) 658.2 (5), 508.3 (10), 375.2 (3), 255.1 (20), 254.6 (100), 247.6 (8), 194.0 (7). HRMS (ESI): m/z calcd for $[(\text{M} - \text{TfO}^-)^+]$ ($\text{C}_{37}\text{H}_{35}\text{O}_3\text{N}_3\text{F}_3\text{S}$) 658.2346; found 658.2344.

(*E*)-11-(2-(1,2,3,5,6,7-Hexahydropyrido[3,2,1-*ij*]quinolin-9-yl)-vinyl)-6,7-dimethyl-4,5,8,9-tetrahydroisoquinolino[1,2-*a*]pyrido[1,2-*k*][2,9]phenanthroline-3,10-dium Trifluoromethanesulfonate (**7**). [6]Helquat dye **7** was prepared and purified in a manner similar to compound **6** using [6]helquat dye precursor **14** (70 mg, 0.103 mmol, 1.0 equiv), 9-julolidine carbaldehyde (147 mg, 0.730 mmol, 7.1 equiv), dry MeOH (7.0 mL), and pyrrolidine (100 μL , 87 mg, 1.217 mmol, 11.8 equiv). The reaction time was 2.5 h. A purple-colored solid was precipitated by addition of Et_2O (56 mL). Reprecipitation was performed three times using MeOH (3 mL) and the addition of Et_2O (24 mL) to form a purple solid. Mp: >350 °C. Yield: 41 mg (46%). ^1H NMR (600 MHz, $(\text{CD}_3)_2\text{CO}$): δ 1.98–2.03 (m, 4H), 2.65 (s, 3H), 2.66 (s, 3H), 2.79–2.83 (m, 4H), 3.30 (ddd, $J = 3.7, 14.2, 17.0$ Hz, 1H), 3.38–3.41 (m, 4H), 3.47 (ddd, $J = 3.7, 14.5, 17.0$ Hz, 1H), 3.80 (ddd, $J = 1.9, 4.7, 17.0$ Hz, 1H), 3.82 (ddd, $J = 1.9, 4.9, 17.0$ Hz, 1H), 5.04 (dt, $J = 3.7, 14.0$ Hz, 1H), 5.16 (dt, $J = 3.7, 14.3$ Hz, 1H), 5.39 (ddd, $J = 1.9, 4.7,$

14.0 Hz, 1H), 5.60 (ddd, $J = 1.9, 4.9, 13.8$ Hz, 1H), 7.20 (dd, $J = 1.2, 8.0$ Hz, 1H), 7.34 (s, 2H), 7.55 (t, $J = 8.1$ Hz, 1H), 7.73 (d, $J = 15.5$ Hz, 1H), 7.82 (ddd, $J = 1.2, 6.9, 8.8$ Hz, 1H), 7.84 (d, $J = 15.5$ Hz, 1H), 7.98 (ddd, $J = 1.1, 6.9, 8.1$ Hz, 1H), 8.01 (dd, $J = 1.2, 8.2$ Hz, 1H), 8.11 (dq, $J = 0.9, 8.8$ Hz, 1H), 8.28 (d, $J = 8.1$ Hz, 1H), 8.53 (d, $J = 6.8$ Hz, 1H), 9.02 (d, $J = 6.8$ Hz, 1H). ^{13}C NMR (151 MHz, $(\text{CD}_3)_2\text{CO}$): δ 16.7, 16.9, 22.1, 26.2, 26.8, 28.3, 49.6, 50.6, 56.2, 110.1, 122.1, 122.5, 123.6, 123.8, 125.6, 126.9, 126.9, 128.8, 129.1, 129.4, 129.7, 132.5, 136.1, 137.4, 138.6, 139.8, 140.3, 141.7, 141.9, 142.2, 147.0, 147.1, 147.3, 152.0, 156.0. Elemental analysis: (%) calcd for $[\text{C}_{42}\text{H}_{39}\text{F}_6\text{N}_3\text{O}_6\text{S}_2]$ C 58.66, H 4.57, N 4.89; found C 58.42, H 4.88, N 4.40. IR (KBr): $\tilde{\nu}$ 3074, 1627, 1588, 1553, 1524, 1484, 1260, 1163, 1030, 638, 573, 517. MS (ESI): m/z (%) 710.4 (14), 561.4 (8), 475.4 (6), 453.4 (10), 362.3 (7), 280.7 (100), 217.1 (4). HRMS (ESI): m/z calcd for $[(\text{M} - \text{TfO}^-)^+]$ ($\text{C}_{41}\text{H}_{39}\text{N}_3\text{O}_3\text{F}_3\text{S}$) 710.2659; found 710.2653.

(*E*)-11-(2-(6-(Dimethylamino)naphthalen-2-yl)vinyl)-6,7-dimethyl-4,5,8,9-tetrahydroisoquinolino[1,2-*a*]pyrido[1,2-*k*][2,9]phenanthroline-3,10-dium Trifluoromethanesulfonate (**8**). [6]-Helquat dye **8** was prepared and purified in manner similar to compound **6** using [6]helquat dye precursor **14** (75 mg, 0.111 mmol, 1.0 equiv), 6-dimethylaminonaphthalaldehyde (66 mg, 0.331 mmol, 3.0 equiv), dry MeOH (7.5 mL), and pyrrolidine (107 μL , 93 mg, 1.302 mmol, 11.7 equiv). A red-colored solid precipitated after the addition of Et_2O (60 mL). Reprecipitation was performed three times using MeOH (10 mL) to form a dark red solid. Mp: >350 °C. Yield: 71 mg (75%). ^1H NMR (600 MHz, CD_3CN): δ 2.53 (s, 3H), 2.55 (s, 3H), 3.05 (ddd, $J = 4.9, 14.3, 17.1$ Hz, 1H), 3.11 (s, 6H), 3.16 (ddd, $J = 4.6, 14.6, 17.2$ Hz, 1H), 3.54 (ddd, $J = 1.8, 3.5, 17.2$ Hz, 1H), 3.58 (ddd, $J = 1.9, 3.8, 17.1$ Hz, 1H), 4.70 (dt, $J = 3.8, 14.0$ Hz, 1H), 4.79 (dt, $J = 3.5, 14.3$ Hz, 1H), 5.01 (ddd, $J = 1.8, 4.6, 13.9$ Hz, 1H), 5.38 (ddd, $J = 1.9, 4.9, 13.8$ Hz, 1H), 6.82 (dd, $J = 1.3, 8.0$ Hz, 1H), 7.01 (d, $J = 2.6$ Hz, 1H), 7.27 (dd, $J = 2.6, 9.1$ Hz, 1H), 7.49 (t, $J = 8.1$ Hz, 1H), 7.58 (d, $J = 15.8$ Hz, 1H), 7.65 (ddd, $J = 1.3, 6.9, 8.8$ Hz, 1H), 7.74 (d, $J = 15.8$ Hz, 1H), 7.77 (d, $J = 8.7$ Hz, 1H), 7.80 (dq, $J = 1.0, 8.8$ Hz, 1H), 7.82 (d, $J = 9.1$ Hz, 1H), 7.83 (dd, $J = 1.3, 8.3$ Hz, 1H), 7.86 (dd, $J = 2.0, 8.7$ Hz, 1H), 7.88 (ddd, $J = 1.1, 6.9, 8.1$ Hz, 1H), 8.03 (d, $J = 2.1$ Hz, 1H), 8.12 (d, $J = 8.1$ Hz, 1H), 8.30 (d, $J = 6.7$ Hz, 1H), 8.60 (d, $J = 6.7$ Hz, 1H). ^{13}C NMR (151 MHz, CD_3CN): δ 17.1, 17.2, 26.1, 26.8, 40.7, 50.3, 56.1, 106.6, 115.6, 117.7, 123.5, 125.0, 125.2, 126.0, 126.8, 127.1, 128.1, 128.3, 128.6, 128.9, 129.1, 129.3, 131.0, 132.4, 132.8, 136.5, 137.0, 137.9, 138.7, 140.0, 141.1, 142.3, 142.4, 143.1, 146.3, 148.1, 151.4, 151.4, 155.5. Elemental analysis: (%) calcd for $[\text{C}_{42}\text{H}_{37}\text{F}_6\text{N}_3\text{O}_6\text{S}_2]$ C 58.80, H 4.35, N 4.90; found C 58.56, H 4.37, N 4.79. IR (KBr): $\tilde{\nu}$ 3081, 1622, 1599, 1560, 1508, 1484, 1263, 1154, 1031, 639, 573, 518. MS (ESI): m/z (%) 708.5 (68), 559.5 (25), 558.5 (50), 375.3 (7), 279.7 (100), 280.2 (48), 194.2 (7). HRMS (ESI): m/z calcd for $[(\text{M} - \text{TfO}^-)^+]$ ($\text{C}_{41}\text{H}_{37}\text{O}_3\text{N}_3\text{F}_3\text{S}$) 708.2502; found 708.2505.

11-(1*E*,3*E*)-4-(4-(Dimethylamino)phenyl)buta-1,3-dien-1-yl)-6,7-dimethyl-4,5,8,9-tetrahydroisoquinolino[1,2-*a*]pyrido[1,2-*k*][2,9]phenanthroline-3,10-dium Trifluoromethanesulfonate (**9**). [6]-Helquat dye **9** was prepared and purified similarly to compound **6** using [6]helquat dye precursor **14** (100 mg, 0.148 mmol, 1.0 equiv), 4-dimethylaminocinnamaldehyde (78 mg, 0.445 mmol, 3.0 equiv), dry MeOH (10.0 mL), and pyrrolidine (143 μL , 124 mg, 1.741 mmol, 11.8 equiv). The reaction time was 0.5 h. The addition of Et_2O (80 mL) gave a purple-colored precipitate. Reprecipitation was performed three times using MeOH (5 mL) and the addition of Et_2O (40 mL) to form a purple solid. Mp: >350 °C. Yield: 72 mg (58%). ^1H NMR (600 MHz, $(\text{CD}_3)_2\text{CO}$): δ 2.66 (s, 3H), 2.67 (s, 3H), 3.10 (s, 6H), 3.48 (ddd, $J = 4.8, 14.4, 17.1$ Hz, 1H), 3.51 (ddd, $J = 4.5, 14.5, 17.0$ Hz, 1H), 3.81 (ddd, $J = 1.9, 3.8, 17.0$ Hz, 1H), 3.86 (ddd, $J = 1.9, 3.6, 17.1$ Hz, 1H), 5.07 (dt, $J = 3.6, 14.0$ Hz, 1H), 5.18 (dt, $J = 3.8, 13.8$ Hz, 1H), 5.40 (ddd, $J = 1.9, 4.5, 14.0$ Hz, 1H), 5.60 (ddd, $J = 1.9, 4.8, 13.6$ Hz, 1H), 6.82–6.84 (m, 2H), 7.16 (d, $J = 15.3$ Hz, 1H), 7.21 (dd, $J = 10.0, 15.3$ Hz, 1H), 7.30 (dd, $J = 1.3, 7.9$ Hz, 1H), 7.34 (d, $J = 14.9$ Hz, 1H), 7.52–7.55 (m, 2H), 7.61 (t, $J = 8.1$ Hz, 1H), 7.74 (dd, $J = 10.0, 14.9$ Hz, 1H), 7.81 (ddd, $J = 1.2, 6.9, 8.8$ Hz, 1H), 8.00 (ddd, $J = 1.1, 6.9, 8.1$ Hz, 1H), 8.04 (dd, $J = 1.3, 8.3$ Hz, 1H), 8.14 (dq, $J = 0.9, 8.8$ Hz, 1H), 8.29 (d, $J = 8.1$ Hz, 1H), 8.55 (d, $J = 6.7$ Hz, 1H), 9.03 (d, $J = 6.7$ Hz, 1H). ^{13}C NMR (151 MHz, $(\text{CD}_3)_2\text{CO}$): δ 16.8, 16.9, 26.2, 26.9, 40.2, 49.8, 56.3, 113.0, 117.6, 123.6, 123.7, 124.4, 124.7, 125.8, 127.0, 128.0, 128.8, 129.2, 129.2, 130.4, 132.5,

136.2, 137.5, 138.6, 140.0, 140.7, 141.9, 142.5, 142.7, 145.1, 147.6, 147.9, 152.0, 152.9, 155.3. Elemental analysis: (%) calcd for $[C_{40}H_{37}F_6N_3O_6S_2]$ C 57.62, H 4.47, N 5.04; found: C 57.11, H 4.78, N 5.11. IR (KBr): $\tilde{\nu}$ 3076, 1626, 1583, 1552, 1527, 1483, 1263, 1153, 1031, 638, 573, 518. MS (ESI): m/z (%) 684.5 (7), 535.5 (13), 534.5 (40), 402.4 (12), 401.4 (17), 377.3 (10), 362.3 (8), 268.2 (43), 267.7 (100), 194.1 (21). HRMS (ESI): m/z calcd for $[(M - TfO^-)^+]$ ($C_{39}H_{37}O_3N_3F_3S$) 684.2502; found 684.2500.

11-((1*E*,3*E*)-4-(1,2,3,5,6,7-Hexahydropyrido[3,2,1-*ij*]quinolin-9-yl)-buta-1,3-dien-1-yl)-6,7-dimethyl-4,5,8,9-tetrahydroisoquinolino-[1,2-*a*]pyrido[1,2-*k*][2,9]phenanthroline-3,10-dium Trifluoromethanesulfonate (**10**). [6]Helquat dye **10** was prepared and purified similarly to compound **6** using [6]helquat dye precursor **14** (70 mg, 0.103 mmol, 1.0 equiv), (*E*)-3-(1,2,3,5,6,7-hexahydropyrido[3,2,1-*ij*]quinolin-9-yl)acrylaldehyde (70 mg, 0.308 mmol, 3.0 equiv), dry MeOH (7.0 mL), and pyrrolidine (100 μ L, 87 mg, 1.217 mmol, 11.8 equiv). The reaction was completed in 2.5 h. The addition of Et₂O (56 mL) gave a deep blue-colored precipitate. Reprecipitation was performed three times using MeOH (10 mL) and the addition of Et₂O (60 mL) to form a deep blue solid. Mp: >350 °C. Yield: 37 mg (41%). ¹H NMR (600 MHz, (CD₃)₂CO): δ 1.96–2.01 (m, 4H), 2.65 (s, 3H), 2.66 (s, 3H), 2.77 (t, *J* = 6.4 Hz, 4H), 3.32–3.35 (m, 4H), 3.33 (ddd, *J* = 4.8, 14.5, 17.2 Hz, 1H), 3.47 (ddd, *J* = 4.6, 14.2, 17.0 Hz, 1H), 3.80 (ddd, *J* = 1.8, 3.5, 17.0 Hz, 1H), 3.84 (ddd, *J* = 1.9, 3.5, 17.2 Hz, 1H), 5.04 (dt, *J* = 3.5, 14.2 Hz, 1H), 5.16 (dt, *J* = 3.5, 14.0 Hz, 1H), 5.39 (ddd, *J* = 1.8, 4.6, 13.8 Hz, 1H), 5.55 (ddd, *J* = 1.9, 4.8, 13.9 Hz, 1H), 7.05 (d, *J* = 15.1 Hz, 1H), 7.08 (d, *J* = 0.6 Hz, 2H), 7.14 (ddd, *J* = 0.7, 10.7, 15.1 Hz, 1H), 7.26 (dd, *J* = 1.3, 7.9 Hz, 1H), 7.26 (d, *J* = 14.8 Hz, 1H), 7.59 (t, *J* = 8.1 Hz, 1H), 7.74 (dd, *J* = 10.7, 14.8 Hz, 1H), 7.80 (ddd, *J* = 1.3, 7.0, 8.8 Hz, 1H), 8.00 (ddd, *J* = 1.1, 7.0, 8.1 Hz, 1H), 8.01 (dd, *J* = 1.3, 8.4 Hz, 1H), 8.13 (dq, *J* = 0.9, 8.8 Hz, 1H), 8.29 (ddt, *J* = 0.7, 1.3, 8.1 Hz, 1H), 8.54 (dd, *J* = 0.9, 6.7 Hz, 1H), 9.03 (d, *J* = 6.7 Hz, 1H). ¹³C NMR (151 MHz, (CD₃)₂CO): δ 16.8, 16.9, 22.3, 26.1, 26.8, 28.3, 49.5, 50.5, 56.2, 116.4, 121.3, 122.1, 122.6, 123.6, 124.1, 125.7, 126.9, 127.5, 128.2, 128.8, 129.1, 129.2, 132.5, 136.1, 137.4, 138.5, 139.8, 140.4, 141.7, 142.2, 142.3, 145.9, 145.9, 147.6, 147.9, 151.9, 155.2. Elemental analysis: (%) calcd for $[C_{44}H_{41}F_6N_3O_6S_2]$ C 59.65, H 4.66, N 4.74; found C 59.48, H 4.30, N 4.12. IR (KBr): $\tilde{\nu}$ 3074, 1627, 1588, 1553, 1524, 1484, 1260, 1163, 1030, 638, 573, 517. MS (ESI) m/z : 736.3 (43), 586.4 (42), 401.2 (11), 294.2 (50), 293.7 (100), 279.7 (22), 194.1 (22), 186.2 (8). HRMS (ESI): m/z calcd for $[(M - TfO^-)^+]$ ($C_{43}H_{41}F_3N_3O_3S$) 736.2815; found 736.2812.

Hyper-Rayleigh Scattering. General details of the HRS experiment have been discussed elsewhere,¹⁹ and the apparatus and experimental procedures used for the fs studies were exactly as described previously.¹¹ These measurements were carried out in MeCN, and the reference compound was crystal violet (octupolar $\beta_{yyy,800} = 500 \times 10^{-30}$ esu in MeCN; from the value of 340×10^{-30} esu in MeOH corrected for local field factors at optical frequencies). For all measurements, dilute solutions ($1-5 \times 10^{-5}$ M) were used to ensure a linear dependence of $I_{2\omega}/I_{\omega}^2$ on concentration, precluding the need for Lambert–Beer correction factors. The absence of demodulation at 800 nm, i.e., constant values of β versus frequency, confirmed that no fluorescence contributions to the HRS signals were present at 400 nm for most of the compounds. Some fluorescence was detected for salts **2** and **6–8**, but this has been accounted for by the data processing protocol used. The reported β values are the averages taken from measurements at different amplitude modulation frequencies (80, 160, and 240 MHz and also 320 MHz in some cases).

Stark Spectroscopy. The Stark apparatus, experimental methods, and data collection procedure were as previously reported,²⁰ except that a Xe arc lamp was used as the light source instead of a W filament bulb. The Stark spectrum for each compound was measured at least twice. The data analysis was carried out as previously described²⁰ by using the zeroth, first, and second derivatives of the absorption spectrum for analysis of the Stark $\Delta\epsilon(\nu)$ spectrum in terms of the Liptay treatment.¹⁵ The dipole-moment change, $\Delta\mu_{12} = \mu_e - \mu_g$, where μ_e and μ_g are the excited and ground-state dipole moments, respectively, was then calculated from the coefficient of the second derivative component. PrCN was used as the glassing medium for which the local field correction f_{int} is estimated as 1.33. The value of the transition dipole-

moment μ_{12} can be determined from the oscillator strength f_{os} of the transition by eq 1.

$$|\mu_{12}| = \left(\frac{f_{os}}{1.08 \times 10^{-5} E_{max}} \right)^{1/2} \quad (1)$$

where E_{max} is the energy of the ICT maximum (in wavenumbers) and μ_{12} is in eÅ. The latter is converted to Debye units by multiplying by 4.803. If the hyperpolarizability β_0 tensor has only nonzero elements along the ICT direction, then this quantity is given by eq 2.

$$\beta_0 = \frac{3\Delta\mu_{12}(\mu_{12})^2}{(E_{max})^2} \quad (2)$$

A relative error of $\pm 20\%$ is estimated for the β_0 values derived from the Stark data and using eq 2, whereas experimental errors of $\pm 10\%$ are estimated for μ_{12} and $\Delta\mu_{12}$. Note that the $\pm 20\%$ uncertainty for the β_0 values is merely statistical and does not account for any errors introduced by two-state extrapolation.

Theoretical Studies. DFT calculations were performed using the Gaussian 09 program package.²¹ The geometries of cations **1'**, **6'**, and DAS⁺ were optimized in the gas phase by using their X-ray crystal structures as starting points.²² The solvent effect of MeCN in the TD-DFT calculations was accounted for by using a CPCM,²³ and the UV–vis absorption spectra were simulated by using the GaussSum program²⁴ (curve fwhm = 3000 cm⁻¹).

Cation **1'** was optimized, and subsequent TD-DFT calculations were carried out using three different functionals (B3LYP,²⁵ M06,²⁶ and CAM-B3LYP²⁷) with the 6-311G(d) basis set. As shown in Figure S1, the visible absorption band contains two transitions when using B3LYP or M06, whereas CAM-B3LYP predicts the UV–vis spectrum more accurately. In all cases, the calculations overestimate the energy of the visible band. Selected frontier MOs of **1'** and **6'** are depicted in Figures S2 and S3, the computed TD-DFT transitions are shown in Table S1 and optimized atomic coordinates in Tables S2 and S3. Static first hyperpolarizabilities calculated for **1'** in the gas phase and MeCN by using 6-311G(d) with B3LYP, M06, or CAM-B3LYP are shown in Table S4. The optimized structures of **1'**, **6'**, and the DAS⁺ cation are included in Figure S4 along with the axis convention used.

■ ASSOCIATED CONTENT

Supporting Information

The Supporting Information is available free of charge on the ACS Publications website at DOI: 10.1021/acs.joc.5b02692.

¹H, and ¹³C NMR spectra of all new compounds, crystallographic and theoretical data (PDF)
CIF file (CCDC 1012247) (CIF)
CIF file (CCDC 1410502) (CIF)

■ AUTHOR INFORMATION

Corresponding Authors

*E-mail: b.coe@manchester.ac.uk.

*E-mail: teply@uochb.cas.cz.

Notes

The authors declare no competing financial interest.

■ ACKNOWLEDGMENTS

This work was supported by ASCR (RVO: 61388963, M200551208 to F.T.), the Czech Science Foundation (13-19213S to F.T.), the Fund for Scientific Research-Flanders (Research Grant 1510712N), the University of Leuven (GOA/2011/03), and the EPSRC (grants EP/G020299/1 and EP/J018635/1 to B.J.C.). B.S.B. acknowledges the Beckman Institute of the California Institute of Technology for support. We thank Mrs. J. Bařinková for her skillful experimental help.

REFERENCES

- (1) *Nonlinear Optical Properties of Matter: From Molecules to Condensed Phases*; Papadopoulos, M. G.; Leszczynski, J.; Sadlej, A. J., Eds.; Springer: Dordrecht, 2006.
- (2) Selected examples: (a) Jeong, J.-H.; Kang, B.-J.; Kim, J.-S.; Jazbinsek, M.; Lee, S.-H.; Lee, S.-C.; Baek, I.-H.; Yun, H.; Kim, J.; Lee, Y. S.; Lee, J.-H.; Kim, J.-H.; Rotermund, F.; Kwon, O.-P. *Sci. Rep.* **2013**, *3*, 3200. (b) McEntee, J. *Chem. World*, 2007; March, pp 52–56. (c) www.teraview.com.
- (3) Concerning DAST: (a) Marinotto, D.; Lucenti, E.; Scavia, G.; Ugo, R.; Tavazzi, S.; Mattei, G.; Cariati, E. *J. Mater. Chem. C* **2014**, *2*, 8532–8538. (b) Zheng, M.-L.; Fujita, K.; Chen, W.-Q.; Duan, X.-M.; Kawata, S. *J. Phys. Chem. C* **2011**, *115*, 8988–8993. (c) Macchi, R.; Cariati, E.; Marinotto, D.; Roberto, D.; Tordin, E.; Ugo, R.; Bozio, R.; Cozzuol, M.; Pedron, D.; Mattei, G. *J. Mater. Chem.* **2010**, *20*, 1885–1890. (d) www.rainbowphotonics.com.
- (4) Compounds like DAST: (a) Kim, J.-S.; Jeong, J.-H.; Yun, H.; Jazbinsek, M.; Kim, J. W.; Rotermund, F.; Kwon, O.-P. *Cryst. Growth Des.* **2013**, *13*, 5085–5091. (b) Kim, P.-J.; Jeong, J.-H.; Jazbinsek, M.; Choi, S.-B.; Baek, I.-H.; Kim, J.-T.; Rotermund, F.; Yun, H.; Lee, Y. S.; Günter, P.; Kwon, O.-P. *Adv. Funct. Mater.* **2012**, *22*, 200–209. (c) Nunzi, F.; Fantacci, S.; Cariati, E.; Tordin, E.; Casati, N.; Macchi, P. *J. Mater. Chem.* **2010**, *20*, 7652–7660. (d) Figi, H.; Mutter, L.; Hunziker, C.; Jazbinsek, M.; Günter, P.; Coe, B. J. *J. Opt. Soc. Am. B* **2008**, *25*, 1786–1793. (e) Coe, B. J.; Harris, J. A.; Hall, J. J.; Brunshwig, B. S.; Hung, S.-T.; Libaers, W.; Clays, K.; Coles, S. J.; Horton, P. N.; Light, M. E.; Hursthouse, M. B.; Garín, J.; Orduna, J. *Chem. Mater.* **2006**, *18*, 5907–5918.
- (5) (a) Coe, B. J.; Fielden, J.; Foxon, S. P.; Asselberghs, I.; Clays, K.; Van Cleuvenbergen, S.; Brunshwig, B. S. *Organometallics* **2011**, *30*, 5731–5743. (b) Coe, B. J.; Fielden, J.; Foxon, S. P.; Helliwell, M.; Brunshwig, B. S.; Asselberghs, I.; Clays, K.; Olesiak, J.; Matczyszyn, K.; Samoc, M. *J. Phys. Chem. A* **2010**, *114*, 12028–12041. (c) Coe, B. J.; Fielden, J.; Foxon, S. P.; Harris, J. A.; Helliwell, M.; Brunshwig, B. S.; Asselberghs, I.; Clays, K.; Garín, J.; Orduna, J. *J. Am. Chem. Soc.* **2010**, *132*, 10498–10512. (d) Coe, B. J.; Harris, J. A.; Brunshwig, B. S.; Garín, J.; Orduna, J. *J. Am. Chem. Soc.* **2005**, *127*, 3284–3285.
- (6) Verbiest, T.; Elshocht, S. V.; Kauranen, M.; Hellemans, L.; Snauwaert, J.; Nuckolls, C.; Katz, T. J.; Persoons, A. *Science* **1998**, *282*, 913–915.
- (7) Recent selected reviews on helicenes and their congeners: (a) Gingras, M. *Chem. Soc. Rev.* **2013**, *42*, 1051–1095. (b) Shen, Y.; Chen, C. F. *Chem. Rev.* **2012**, *112*, 1463–1535. (c) Stará, I. G.; Starý, I. In *Science of Synthesis*; Siegel, J. S., Tobe, Y., Eds.; Thieme: Stuttgart, 2010; Vol. 45, pp 885–953. (d) Rajca, A.; Miyasaka, M. In *Functional Organic Materials*; Müller, T. J. J., Bunz, U. H. F., Eds.; Wiley-VCH: Weinheim, 2007; pp 547–581.
- (8) (a) Torricelli, F.; Bosson, J.; Besnard, C.; Chekini, M.; Bürgi, T.; Lacour, J. *Angew. Chem., Int. Ed.* **2013**, *52*, 1796–1800. (b) Herse, C.; Bas, D.; Krebs, F. C.; Bürgi, T.; Weber, J.; Wesolowski, T.; Laursen, B. W.; Lacour, J. *Angew. Chem., Int. Ed.* **2003**, *42*, 3162–3166. (c) Bosson, J.; Gouin, J.; Lacour, J. *Chem. Soc. Rev.* **2014**, *43*, 2824–2840.
- (9) Racemic Arai's dyes have been mentioned only in a review, and synthetic procedures and other details have not been published. See: Sato, K.; Arai, S. In *Cyclophane Chemistry for the 21st Century*, Takemura, H., Ed.; Research Signpost: Trivandrum, 2002; p 173 (see p 192).
- (10) (a) Reyes-Gutiérrez, P. E.; Jirásek, M.; Severa, L.; Novotná, P.; Koval, D.; Sázelová, P.; Vávra, J.; Meyer, A.; Císařová, I.; Šaman, D.; Pohl, R.; Štěpánek, P.; Slaviček, P.; Coe, B. J.; Hájek, M.; Kašička, V.; Urbanová, M.; Teplý, F. *Chem. Commun.* **2015**, *51*, 1583–1586. Further selected reports on helquats: (b) Adriaenssens, L.; Severa, L.; Šalová, T.; Císařová, I.; Pohl, R.; Šaman, D.; Rocha, S. V.; Finney, N. S.; Pospíšil, L.; Slaviček, P.; Teplý, F. *Chem. - Eur. J.* **2009**, *15*, 1072–1076. (c) Pospíšil, L.; Bednářová, L.; Štěpánek, P.; Slaviček, P.; Vávra, J.; Hromadová, M.; Dlouhá, H.; Tarábek, J.; Teplý, F. *J. Am. Chem. Soc.* **2014**, *136*, 10826–10829. (d) Vávra, J.; Severa, L.; Císařová, I.; Klepetářová, B.; Šaman, D.; Koval, D.; Kašička, V.; Teplý, F. *J. Org. Chem.* **2013**, *78*, 1329–1342.
- (11) Olbrechts, G.; Clays, K.; Persoons, A. *J. Opt. Soc. Am. B* **2000**, *17*, 1867–1873.
- (12) (a) Oudar, J. L.; Chemla, D. S. *J. Chem. Phys.* **1977**, *66*, 2664–2668. (b) Oudar, J. L. *J. Chem. Phys.* **1977**, *67*, 446–457.
- (13) (a) Clays, K.; Coe, B. J. *Chem. Mater.* **2003**, *15*, 642–648. (b) Coe, B. J.; Harris, J. A.; Asselberghs, I.; Wostyn, K.; Clays, K.; Persoons, A.; Brunshwig, B. S.; Coles, S. J.; Gelbrich, T.; Light, M. E.; Hursthouse, M. B.; Nakatani, K. *Adv. Funct. Mater.* **2003**, *13*, 347–357.
- (14) Coe, B. J.; Foxon, S. P.; Harper, E. C.; Harris, J. A.; Helliwell, M.; Raftery, J.; Asselberghs, I.; Clays, K.; Franz, E.; Brunshwig, B. S.; Fitch, A. G. *Dyes Pigm.* **2009**, *82*, 171–186.
- (15) (a) Bublitz, G. U.; Boxer, S. G. *Annu. Rev. Phys. Chem.* **1997**, *48*, 213–242. (b) Liptay, W. In *Excited States*; Lim, E. C., Ed.; Academic Press: New York, 1974; Vol. 1, pp 129–229.
- (16) Coe, B. J.; Pilkington, R. A. *J. Phys. Chem. A* **2014**, *118*, 2253–2268.
- (17) Coe, B. J.; Helliwell, M.; Peers, M. K.; Raftery, J.; Rusanova, D.; Clays, K.; Depotter, G.; Brunshwig, B. S. *Inorg. Chem.* **2014**, *53*, 3798–3811.
- (18) Amabilino, D. B.; Ashton, P. R.; Reder, A. S.; Spencer, N.; Stoddart, J. F. *Angew. Chem., Int. Ed. Engl.* **1994**, *33*, 1286–1290.
- (19) (a) Hendrickx, E.; Clays, K.; Persoons, A. *Acc. Chem. Res.* **1998**, *31*, 675–683. (b) Clays, K.; Persoons, A. *Rev. Sci. Instrum.* **1992**, *63*, 3285–3289.
- (20) (a) Coe, B. J.; Harris, J. A.; Brunshwig, B. S. *J. Phys. Chem. A* **2002**, *106*, 897–905. (b) Shin, Y. K.; Brunshwig, B. S.; Creutz, C.; Sutin, N. *J. Phys. Chem.* **1996**, *100*, 8157–8169.
- (21) Frisch, M. J.; et al. *Gaussian 09*, revision B.01; Gaussian, Inc.: Wallingford, CT, 2010.
- (22) Structures for several salts of DAS⁺: Sun, Z.-H.; Liu, X.-T.; Wang, X.-Q.; Li, L.-N.; Shi, X.-J.; Li, S.-G.; Ji, C.-M.; Luo, J.-H.; Hong, M.-C. *Cryst. Growth Des.* **2012**, *12*, 6181–6197.
- (23) (a) Cossi, M.; Rega, N.; Scalmani, G.; Barone, V. *J. Comput. Chem.* **2003**, *24*, 669–681. (b) Barone, V.; Cossi, M. *J. Phys. Chem. A* **1998**, *102*, 1995–2001.
- (24) O'Boyle, N. M.; Tenderholt, A. L.; Langner, K. M. *J. Comput. Chem.* **2008**, *29*, 839–845.
- (25) Becke, A. D. *J. Chem. Phys.* **1993**, *98*, 5648–5652.
- (26) Zhao, Y.; Truhlar, D. *Theor. Chem. Acc.* **2008**, *120*, 215–241.
- (27) Yanai, T.; Tew, D. P.; Handy, N. C. *Chem. Phys. Lett.* **2004**, *393*, 51–57.